

# Nanocrystalline Intermetallics and Alloys

Dingsheng Wang, Qing Peng, and Yadong Li (✉)

Department of Chemistry, Tsinghua University, Beijing 100084, China

Received: 24 June 2010 / Accepted: 27 June 2010

© The Author(s) 2010. This article is published with open access at Springerlink.com

## ABSTRACT

Nanocrystalline intermetallics and alloys are novel materials with high surface areas which are potential low-cost and high-performance catalysts. Here, we report a general approach to the synthesis of a large variety of nanocrystalline intermetallics and alloys with controllable composition, size, and morphology: these include Au-, Pd-, Pt-, Ir-, Ru-, and Rh-based bi- or tri-metallic nanocrystals. We find that only those intermetallics and alloys whose effective electronegativity is larger than a critical value (1.93) can be prepared by co-reduction in our synthetic system. Our methodology provides a simple and convenient route to a variety of intermetallic and alloyed nanomaterials which are promising candidates for catalysts for reactions such as methanol oxidation, hydroformylation, the Suzuki reaction, cyclohexene hydroconversion, and the selective hydrogenation of acetylene.

## KEYWORDS

Intermetallics, alloys, nanocrystals, controllable synthesis, catalysts

Since the discovery of intermetallic compounds of the type  $MNi_5$  ( $M = Th, U$ , or  $Zr$ ) which perform as effective methanation catalysts [1], intermetallics, and alloys have emerged as a class of novel materials which provide great opportunities for the development of low-cost and high-performance industrial catalysts [2–8]. Intermetallics and alloys are traditionally synthesized using metallurgical techniques which require high-temperature heating and annealing for long periods of time [9, 10]. Via these strategies, it is difficult to obtain nanocrystalline intermetallics and alloys with the high surface areas which are urgently needed in various applied fields such as energy, environment, and catalysis [11, 12]. As early as 1926, Raney Ni with a high surface area was prepared via selective leaching of nickel–aluminium alloys by

Murray Raney [13]. However, design of facile and general strategies for the synthesis of other intermetallics and alloys with high surface areas still remains a great challenge. Undoubtedly, the emergence and development of nanoscience and nanotechnology offer new opportunities in this area [14–18].

Recently, we developed a general strategy for the synthesis of various nanocrystals, whereby noble metal ions can be reduced to monodisperse noble metal nanocrystals by a mixture of ethanol and linoleic acid [19]. However, attempts to synthesize intermetallics and alloys of noble and non-noble metals (e.g., FePt, NiPt, and CoPd) with this strategy were unsuccessful, mainly due to the low reducing power of ethanol and linoleic acid. On the other hand, we found that with strong reducing agents such as  $NaBH_4$  and  $N_2H_4$ , the

Address correspondence to ydli@mail.tsinghua.edu.cn

difference in electron affinities of the transition and noble metals dominates the reduction process. As a result, it becomes difficult to precisely control the nucleation and growth process to obtain intermetallics and alloys, and core–shell structures tend to form instead. Therefore, in order to obtain novel intermetallic or alloy-based low-cost catalysts, developing a system to achieve co-reduction of different metals as well as precise control of nucleation and growth processes is of critical importance.

Very recently, we exploited an effective single-component-system for the preparation of mono-disperse Ag nanoparticles using  $\text{AgNO}_3$  as the starting material. Here octadecylamine (ODA) functions simultaneously as solvent, surfactant, and reducing agent [20]. Au, Pd, Pt, Ir, Ru, and Rh nanocrystals can also be synthesized in this system. However, when we used transition metal inorganic salts (e.g.,  $\text{Ni}(\text{NO}_3)_2$ ,  $\text{Co}(\text{NO}_3)_2$ ,  $\text{Zn}(\text{NO}_3)_2$ , etc.) as precursors, we found that the corresponding metal oxide nanocrystals were obtained instead of the metals [21]. When two kinds of metal ions ( $\text{Ag}^+$ ,  $\text{Au}^{3+}$ ,  $\text{Pt}^{4+}$ ,  $\text{Pd}^{2+}$ ,  $\text{Ni}^{2+}$ ,  $\text{Co}^{2+}$ ,  $\text{Zn}^{2+}$ ) were added together in the ODA system, we found that some could be co-reduced to alloys and intermetallics while others could not be reduced. Why couldn't transition metal ions (e.g.,  $\text{Ni}^{2+}$ ,  $\text{Co}^{2+}$ ,  $\text{Zn}^{2+}$ , etc.) be reduced in this system? Why could some metal ions be co-reduced by ODA while others couldn't? Intrigued by these phenomena, we decided to further explore the underlying chemistry. It is well known that electronegativity is a measure of the ability of a chemically bonded atom to attract electrons, and one scale of electronegativity was devised by Pauling in 1932 [22]. The electronegativity of Ag (1.93) is the lowest of all the noble metals, but is still larger than that of transition metals (e.g., Ni (1.91), Co (1.88), and Zn (1.65), see Table 1). In our ODA synthesis system, only metals with electronegativities greater than or equal to that of Ag (1.93) can be reduced. Is 1.93 the critical electronegativity for metal reduction in our system, below which reduction of metal ions becomes impossible? These issues deserve to be studied further.

Which intermetallics and alloys can be synthesized in our ODA system? We suppose that nanocrystalline intermetallics and alloys can be regarded as artificial

metal atoms (AMA). There exist metal–metal bonds within, or on the surface of, intermetallics and alloy particles. These particles should have the ability to attract electrons to themselves just as single metal atoms do, and therefore we can define an electronegativity for them [5]. Here, we propose a new concept for bi- or multimetallics, that is, effective electronegativity ( $\chi_{\text{effective}}$ ).  $\chi_{\text{effective}}$  is determined by the electronegativity of the component metals and the value is given by the following equation:

$$\chi_{\text{effective}}(M_x M'_y) = \frac{x}{x+y} \chi_M + \frac{y}{x+y} \chi_{M'} \quad (1)$$

Based on the above formula, we calculate the effective electronegativity of some bi- or tri-metallics and summarize the results in Table 1.

According to the calculated results,  $\chi_{\text{effective}}$  of most AMAs is larger than 1.93, indicating that it should be possible to prepare them by reduction with ODA. In order to test this hypothesis, we designed the following experiments.

Firstly, we selected some representative intermetallics (with the values of  $\chi_{\text{effective}}$  all greater than 1.93, as shown in parentheses) such as InPd (1.99), CuIr (2.05), NiRu (2.06), FeRh (2.06), CoRh (2.08), CoPd<sub>2</sub> (2.09), NiPt (2.1), NiRh (2.1), ZnPt<sub>3</sub> (2.12), CdPt<sub>3</sub> (2.13), InPt<sub>3</sub> (2.16), and CoPt<sub>3</sub> (2.18) as possible target products of co-reduction in the ODA system. We carried out experiments according to the pre-designed protocol using mixtures of inorganic salts corresponding to the above intermetallics and characterized the as-obtained products (for example, a 3:1 molar ratio of  $\text{H}_2\text{PtCl}_6$

**Table 1** Electronegativities of single metals and estimated effective electronegativities of artificial metal atoms

Metal	Ag	Au	Pd	Pt	Ir	Ru	Rh
$\chi_{\text{metal}}^*$	1.93	2.54	2.20	2.28	2.20	2.20	2.28
Metal	Fe	Co	Ni	Cu	Zn	Cd	In
$\chi_{\text{metal}}^*$	1.83	1.88	1.91	1.90	1.65	1.69	1.78
AMA	CuPt	InPt <sub>3</sub>	NiPt	CoPt <sub>3</sub>	FePt	CuPd	ZnPt <sub>3</sub>
$\chi_{\text{effective}}$	2.09	2.16	2.10	2.18	2.06	2.05	2.12
AMA	NiPd	ZnPd	CdPt <sub>3</sub>	InPd	CuAu	AgFe	AgNi
$\chi_{\text{effective}}$	2.06	1.93	2.13	1.99	2.22	1.88	1.92

\*Source: Huheey, J. E. *Inorganic Chemistry: Principles of Structure and Reactivity*; 2nd edition, Harper & Row: New York, 1978.



and  $Zn(NO_3)_2$  was used as the precursor mixture for the attempted synthesis of intermetallic  $ZnPt_3$  nanocrystals).

Figures 1(a) and 2(a), respectively, show powder X-ray diffraction (XRD) patterns and transmission electron microscope (TEM) images of the as-obtained products. The XRD patterns of each of the products matches exactly with the standard pattern of the corresponding intermetallic compounds. These experimental results confirm that the formation of intermetallic compounds whose effective electronegativity is larger than 1.93 can be effected in our ODA system using mixtures of salts of noble metals and transition metals as precursors.

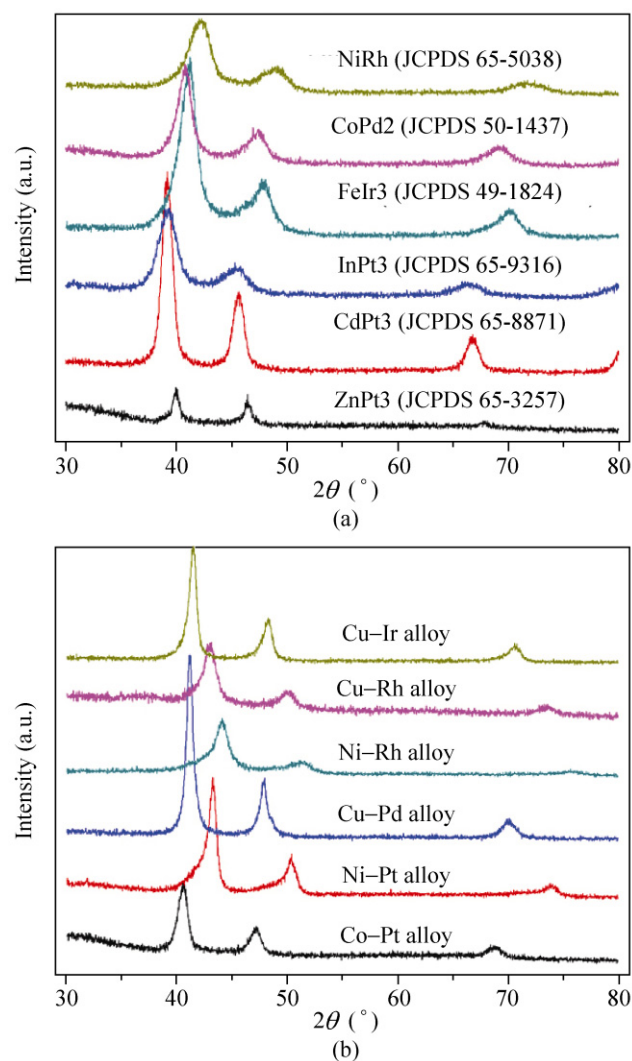


**Figure 1** XRD patterns of as-synthesized (a) intermetallic and (b) alloyed nanocrystals

We then investigated the possibility of forming  $AgFe$  (1.88) and  $AgNi$  (1.92), whose effective electronegativities are smaller than 1.93, by co-reduction in the ODA system. When  $AgNO_3$  and  $Ni(NO_3)_2$  (or  $Fe(NO_3)_3$ ) were used as reactants, no Ag-based intermetallics were formed. The XRD patterns in Figs. 3(a) and 3(b) show that the resulting products are composed of mixtures of Ag and  $NiO$  (or Ag and  $Fe_2O_3$ ). These experimental results further confirm that the 1.93 is a critical minimum effective electronegativity below which intermetallic compounds cannot be prepared by co-reduction.

In order to further investigate the applicability of the proposed rule in alloy synthesis, we attempted to synthesize  $Co_{1-x}Pt_x$ ,  $Cu_{1-x}Pt_x$ ,  $Ni_{1-x}Pt_x$ ,  $Fe_{1-x}Pd_x$ ,  $Co_{1-x}Pd_x$ ,  $Ni_{1-x}Pd_x$ ,  $Zn_{1-x}Pd_x$ , and  $Sn_{1-x}Pd_x$  alloys in our ODA system. The effective electronegativity of these alloys is determined by the value of  $x$ . According to the effective electronegativity rule, there exists a critical value of  $x$  which makes the electronegativity equal to 1.93, namely,  $Co_{0.87}Pt_{0.13}$ ,  $Cu_{0.92}Pt_{0.08}$ ,  $Ni_{0.95}Pt_{0.05}$ ,  $Fe_{0.73}Pd_{0.27}$ ,  $Co_{0.84}Pd_{0.16}$ ,  $Ni_{0.93}Pd_{0.07}$ ,  $Zn_{0.49}Pd_{0.51}$ , and  $Sn_{0.67}Pd_{0.33}$ . Can alloys of  $Co_{1-x}Pt_x$  ( $x \geq 0.13$ ),  $Cu_{1-x}Pt_x$  ( $x \geq 0.08$ ),  $Ni_{1-x}Pt_x$  ( $x \geq 0.05$ ),  $Fe_{1-x}Pd_x$  ( $x \geq 0.27$ ),  $Co_{1-x}Pd_x$  ( $x \geq 0.16$ ),  $Ni_{1-x}Pd_x$  ( $x \geq 0.07$ ),  $Zn_{1-x}Pd_x$  ( $x \geq 0.51$ ), and  $Sn_{1-x}Pd_x$  ( $x \geq 0.33$ ) be synthesized in our ODA system? Figures 1(b) and 2(b), respectively, show XRD patterns and TEM images of the as-obtained products, which confirm that alloys whose effective electronegativity is greater than or equal to 1.93 can indeed be prepared in our ODA system.

Can alloys with an effective electronegativity smaller than 1.93 also be prepared by co-reduction in ODA? When a 4:1 molar ratio of Fe and Pd precursors was reacted in ODA, we were unable to obtain  $Fe_{0.8}Pd_{0.2}$  ( $\chi_{\text{effective}} = 1.90$ ) alloys. The XRD pattern in Fig. 3(c) shows that the products is a mixture of  $FePd$  alloy ( $\chi_{\text{effective}} = 2.02$ ) and  $Fe_3O_4$ , indicating that alloys with effective electronegativity lower than 1.93 cannot be formed by co-reduction of a noble metal salt and a transition metal salt.

We also extended our study to the synthesis of tri-metallic compounds. The calculation of the effective electronegativity of tri-metallic materials is analogous to that for bi-metallic compounds. Figure 4 shows the

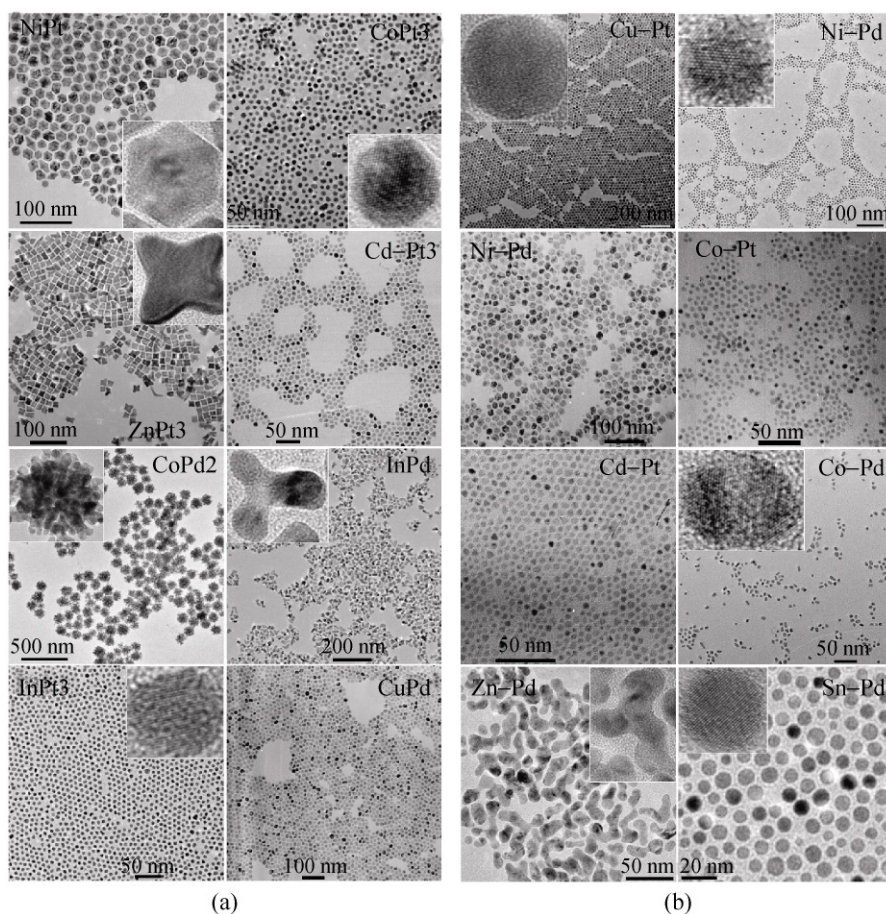


**Figure 2** TEM images of as-synthesized (a) intermetallic and (b) alloyed nanocrystals

XRD pattern and TEM image of the product formed by the reaction between  $\text{Cu}(\text{NO}_3)_2$ ,  $\text{PdCl}_2$ , and  $\text{H}_2\text{PtCl}_6$  in ODA. The reaction yields nearly monodisperse intermetallic  $\text{Cu}_2\text{PdPt}$  ( $\chi_{\text{effective}} = 2.07$ ) nanoparticles. Therefore, the proposed effective electronegativity rule also applies to synthesis of tri-metallic nanocrystals in our ODA system.

All of the above experimental results fully confirm our proposed effective electronegativity rule, namely, we can design rational strategies to synthesize various intermetallics and alloys only if their effective electronegativity is larger than 1.93.

In the ODA system, non-noble metal ions cannot be reduced directly in the absence of noble metal ions. However, noble and non-noble metal ions can be co-reduced by ODA. This is an intriguing phenomenon. Recently, some groups have reported theoretical calculations on bi-metallic materials [23, 24]. For

example, it was shown that the surface atoms of the gold particles formed in an initial reduction step carry slightly negative charges, which facilitates the subsequent adsorption of  $\text{Ag}^+$  cations on the gold particle surface [23, 25]. These may help us to understand the interesting observations in the ODA system, since they suggest that the reduction of a non-noble metal can be induced by the reduction of a noble metal [25].

This process can be illustrated by using PtCu alloy as an example. After  $\text{Pt}^{4+}$  and  $\text{Cu}^{2+}$  ions were added into the ODA solvent at a designated temperature,  $\text{Pt}^{4+}$  ions were first reduced by ODA to form a neutral Pt atom, because the electronegativity of Pt is larger than that of Cu [26]. A positive  $\text{Cu}^{2+}$  ion will attract the electron cloud of the Pt atom and cause it to be polarized towards the positive  $\text{Cu}^{2+}$  center. This would in turn induce a partial positive charge on the opposite side of the Pt atom which accepts electrons donated

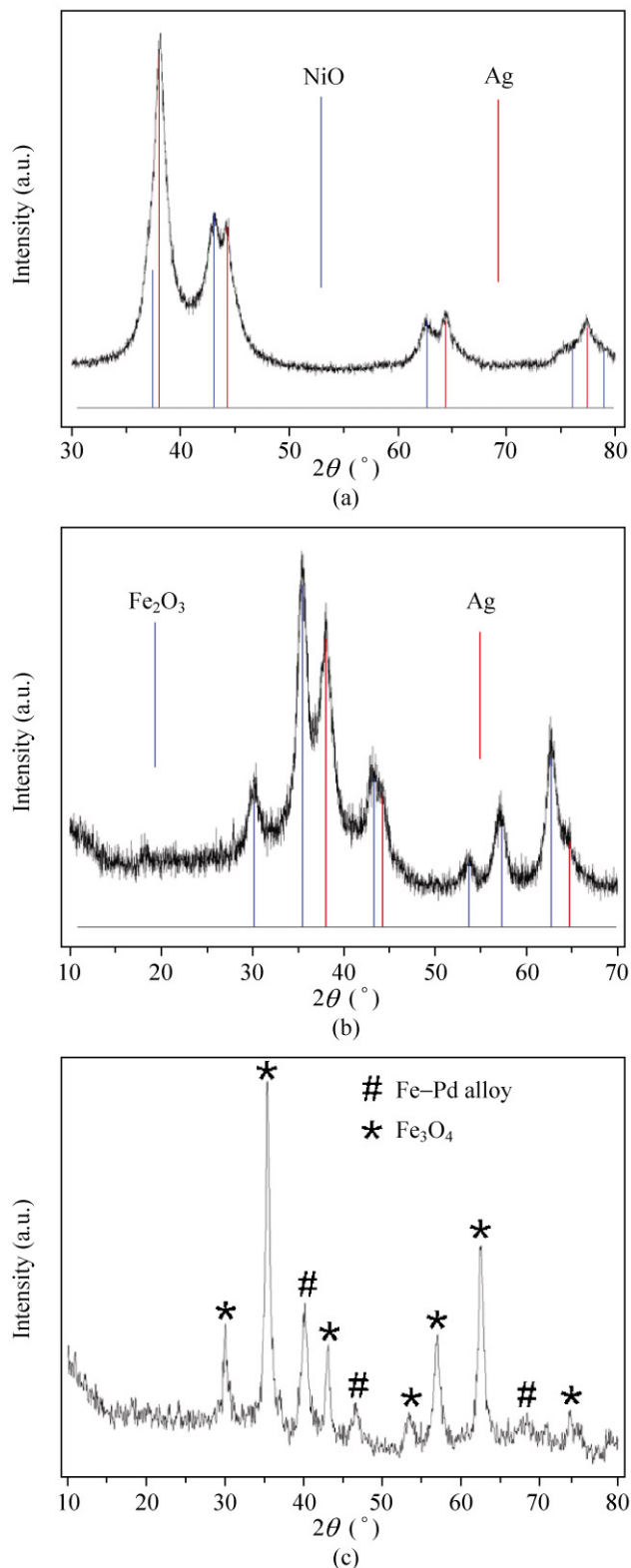


**Figure 3** XRD patterns of (a) Ag and NiO; (b) Ag and  $\text{Fe}_2\text{O}_3$ ; (c) Fe–Pd alloys and  $\text{Fe}_3\text{O}_4$

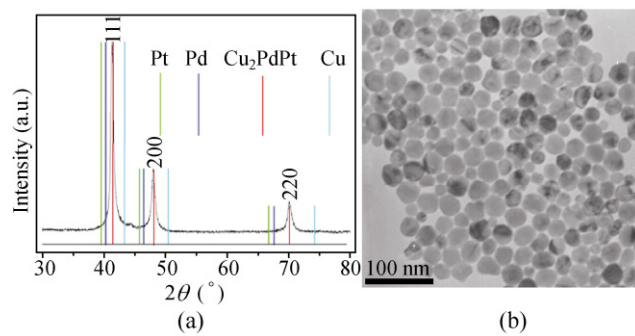


**Figure 4** XRD pattern and TEM image of Cu<sub>2</sub>PdPt nanocrystals

by the ODA reducing agent [25]. The continuous supply of electrons from ODA to Pt results in a concomitant shift in electron density from Pt to Cu until the Cu<sup>2+</sup> ion is reduced completely and a Pt–Cu metal–metal bond formed ( $\chi_{\text{effective}} = 2.10$ ). A similar electron pathway also allows other Pt–Cu alloys to be formed until the  $\chi_{\text{effective}}$  value drops below 1.93 (at a composition Cu<sub>0.92</sub>Pt<sub>0.08</sub>), where the formation of an alloy becomes unfavorable. After nucleation of a CuPt alloy is complete, the subsequent crystal growth process enabled us to obtain nanocrystalline CuPt alloys with controllable shape and size under different synthesis conditions (see Table S-1 and Figs. S-1–S-8 in the Electronic Supplementary Material (ESM) for details).

We also investigated the catalytic properties of the as-synthesized noble-metal-based intermetallic and alloyed nanocrystals obtained using our noble-metal-induced reduction (NMIR) procedure. We took Pt-based intermetallics and alloys as examples and investigated their catalytic activity towards methanol oxidation. Figure S-9 in the ESM shows the cyclic voltammograms recorded for as-obtained intermetallics and alloys in 1 mol/L CH<sub>3</sub>OH with 1 mol/L HClO<sub>4</sub> as the supporting electrolyte. For comparison, the voltammogram for Pt nanocrystals of a similar size is also included. The Ni<sub>0.64</sub>Pt<sub>0.36</sub> alloy displays nearly twice the current density of the pure Pt catalyst (see Figs. S-9–S-11 in the ESM for details). Other Pt-based intermetallics and alloys such as Fe<sub>0.12</sub>Pt<sub>0.88</sub> alloy and InPt<sub>3</sub> intermetallic nanocrystals also appear to be significantly more active for methanol oxidation (Fig. S-9 in the ESM).

In order to further study the catalytic performance of intermetallic and alloy nanocrystals, we selected 1-octene hydroformylation, the Suzuki reaction, the cyclohexene hydroconversion reaction, and the selective hydrogenation of acetylene as probe reactions. The preliminary results (Tables S-2 and S-3, Figs. S-12 and S-13 in the ESM) show that intermetallic and alloyed nanocrystals are indeed active catalysts. Their catalytic performance can be optimized by controlling the composition, size, and morphology of the nanocrystals, and a detailed study is underway in our group.

In summary, we have developed an effective general strategy for the synthesis of nanocrystalline intermetallics and alloys with controllable composition, size, and morphology. An electronegativity rule has been proposed as a guide to the possibility of synthesizing bi- or tri-metallic nanocrystals with a given composition in the ODA system and was verified experimentally. A preliminary study of the catalytic performance of the as-synthesized intermetallic and alloyed nanocrystals in some industrially important reactions indicates that they are promising catalysts for these reactions.

## Acknowledgements

This work was supported by the National Natural Science Foundation of China (NSFC) (No. 90606006), and the State Key Project of Fundamental Research for Nanoscience and Nanotechnology (No. 2006CB932300). We thank Pu Xiao, Prof. Xinping Qiu, Prof. Dehua He, Prof. Dianqing Li, and Prof. Weiguo Song for characterizing the catalytic properties of the products.

**Electronic Supplementary Material:** Supplementary material (experimental procedures, detailed characterization of products, and results of catalytic studies, in Tables S-1–S-3 and Figs. S-1–S-13) is available in the online version of this article at <http://dx.doi.org/10.1007/s12274-010-0018-4> and is accessible free of charge.

**Open Access:** This article is distributed under the terms of the Creative Commons Attribution Noncommercial

License which permits any noncommercial use, distribution, and reproduction in any medium, provided the original author(s) and source are credited.

## References

- [1] Elattar, A.; Takeshita, T.; Wallace, W. E.; Craig, R. S. Intermetallic compounds of the type  $MNi_5$  as methanation catalysts. *Science* **1977**, *196*, 1093–1094.
- [2] Ahmadi, T. S.; Wang, Z. L.; Green, T. C.; Henglein, A.; El-Sayed, M. A. Shape-controlled synthesis of colloidal platinum nanoparticles. *Science* **1996**, *272*, 1924–1926.
- [3] Lim, B.; Jiang, M.; Camargo, P. H. C.; Cho, E. C.; Tao, J.; Lu, X.; Zhu, Y.; Xia, Y. N. Pd–Pt bimetallic nanodendrites with high activity for oxygen reduction. *Science* **2009**, *324*, 1302–1305.
- [4] Taub, A. I.; Fleischer, R. L. Intermetallic compounds for high-temperature structural use. *Science* **1989**, *243*, 616–621.
- [5] Rodriguez, J. A.; Goodman, D. W. The nature of the metal–metal bond in bimetallic surfaces. *Science* **1992**, *257*, 897–903.
- [6] Jaime, M.; Movshovich, R.; Stewart, G. R.; Beyermann, W. P.; Berisso, M. G.; Hundley, M. F.; Canfield, P. C.; Sarrao, J. L. Closing the spin gap in the Kondo insulator  $Ce_3Bi_4Pt_3$  at high magnetic fields. *Nature* **2000**, *405*, 160–163.
- [7] Gschneidner, K.; Russell, A.; Pecharsky, A.; Morris, J.; Zhang, Z. H.; Lograsso, T.; Hsu, D.; Lo, C. H. C.; Ye, Y. Y.; Slager, A.; Kesse, D. A family of ductile intermetallic compounds. *Nat. Mater.* **2003**, *2*, 587–591.
- [8] Krenke, T.; Duman, E.; Acet, M.; Wassermann, E. F.; Moya, X.; Manosa, L.; Planes, A. Inverse magnetocaloric effect in ferromagnetic Ni–Mn–Sn alloys. *Nat. Mater.* **2005**, *4*, 450–454.
- [9] Novet, T.; Johnson, D. C. New synthetic approach to extended solids—selective synthesis of iron silicides via the amorphous state. *J. Am. Chem. Soc.* **1991**, *113*, 3398–3403.
- [10] Suryanarayana, C. Mechanical alloying and milling. *Prog. Mater. Sci.* **2001**, *46*, 1–184.
- [11] Pilani, M. P. The role of soft colloidal templates in controlling the size and shape of inorganic nanocrystals. *Nat. Mater.* **2003**, *2*, 145–150.
- [12] Banin, U. Tiny seeds make a big difference—a seeded-growth approach provides shape-controlled bimetallic nanocrystals and opens the way for a rich selection of new nanoscale building blocks. *Nat. Mater.* **2007**, *6*, 625–626.
- [13] Raney, M. Method of producing finely divided nickel. U.S. Patent 1628190, 1927.



- [14] Habas, S. E.; Lee, H.; Radmilovic, V.; Somorjai, G. A.; Yang, P. Shaping binary metal nanocrystals through epitaxial seeded growth. *Nat. Mater.* **2007**, *6*, 692–697.
- [15] Sun, S. H.; Murray, C. B.; Weller, D.; Folks, L.; Moser, A. Monodisperse FePt nanoparticles and ferromagnetic FePt nanocrystal superlattices. *Science* **2000**, *287*, 1989–1992.
- [16] Lim, B.; Jiang, M. J.; Yu, T.; Camargo, P. H. C.; Xia, Y. N. Nucleation and growth mechanisms for Pd–Pt bimetallic nanodendrites and their electrocatalytic properties. *Nano Res.* **2010**, *3*, 69–80.
- [17] Som, T.; Karmakar, B. Core–shell Au–Ag nanoparticles in dielectric nanocomposites with plasmon-enhanced fluorescence: A new paradigm in antimony glasses. *Nano Res.* **2009**, *2*, 607–616.
- [18] Wang, D. S.; Xie, T.; Li, Y. D. Nanocrystals: Solution-based synthesis and applications as nanocatalysts. *Nano Res.* **2009**, *2*, 30–46.
- [19] Wang, X.; Zhuang, J.; Peng, Q.; Li, Y. D. A general strategy for nanocrystal synthesis. *Nature* **2005**, *437*, 121–124.
- [20] Wang, D. S.; Xie, T.; Peng, Q.; Li, Y. D. Ag, Ag<sub>2</sub>S, and Ag<sub>2</sub>Se nanocrystals: Synthesis, assembly, and construction of mesoporous structures. *J. Am. Chem. Soc.* **2008**, *130*, 4016–4022.
- [21] Wang, D. S.; Xie, T.; Peng, Q.; Zhang, S. Y.; Chen, J.; Li, Y. D. Direct thermal decomposition of metal nitrates in octadecylamine to metal oxide nanocrystals. *Chem. Eur. J.* **2008**, *14*, 2507–2513.
- [22] Pauling, L. The nature of the chemical bond. IV. The energy of single bonds and the relative electronegativity of atoms. *J. Am. Chem. Soc.* **1932**, *54*, 3570–3582.
- [23] Liu, X. Y.; Wang, A. Q.; Yang, X. F.; Zhang, T.; Mou, C. Y.; Su, D. S.; Li, J. Synthesis of thermally stable and highly active bimetallic Au–Ag nanoparticles on inert supports. *Chem. Mater.* **2009**, *21*, 410–418.
- [24] Wang, L. L.; Johnson, D. D. Predicted trends of core–shell preferences for 132 late transition-metal binary-alloy nanoparticles. *J. Am. Chem. Soc.* **2009**, *131*, 14023–14029.
- [25] Wang, D. S.; Li, Y. D. One-pot protocol for Au-based hybrid magnetic nanostructures via a noble-metal-induced reduction process. *J. Am. Chem. Soc.* **2010**, *132*, 6280–6281.
- [26] Zheng, H. M.; Smith, R. K.; Jun, Y. W.; Kisielowski, C.; Dahmen, U.; Alivisatos, A. P. Observation of single colloidal platinum nanocrystal growth trajectories. *Science* **2009**, *324*, 1309–1312.